

BIBLIOGRAPHIC INFORMATION SYSTEM

JOURNAL FULL TITLE: Journal of Biomedical Research & Environmental Sciences

ABBREVIATION (NLM): J Biomed Res Environ Sci **ISSN:** 2766-2276 **WEBSITE:** <https://www.jelsciences.com>

SCOPE & COVERAGE

- ▶ **Sections Covered:** 34 specialized sections spanning 143 topics across Medicine, Biology, Environmental Sciences, and General Science
- ▶ Ensures broad interdisciplinary visibility for high-impact research.

PUBLICATION FEATURES

- ▶ **Review Process:** Double-blind peer review ensuring transparency and quality
- ▶ **Time to Publication:** Rapid 21-day review-to-publication cycle
- ▶ **Frequency:** Published monthly
- ▶ **Plagiarism Screening:** All submissions checked with iThenticate

INDEXING & RECOGNITION

- ▶ **Indexed in:** [Google Scholar](#), IndexCopernicus (**ICV 2022: 88.03**)
- ▶ **DOI:** Registered with CrossRef (**10.37871**) for long-term discoverability
- ▶ **Visibility:** Articles accessible worldwide across universities, research institutions, and libraries

OPEN ACCESS POLICY

- ▶ Fully Open Access journal under Creative Commons Attribution 4.0 License (CC BY 4.0)
- ▶ Free, unrestricted access to all articles globally

GLOBAL ENGAGEMENT

- ▶ **Research Reach:** Welcomes contributions worldwide
- ▶ **Managing Entity:** SciRes Literature LLC, USA
- ▶ **Language of Publication:** English


SUBMISSION DETAILS

- ▶ Manuscripts in Word (.doc/.docx) format accepted

SUBMISSION OPTIONS

- ▶ **Online:** <https://www.jelsciences.com/submit-your-paper.php>
- ▶ **Email:** support@jelsciences.com, support@jbresonline.com

[HOME](#)[ABOUT](#)[ARCHIVE](#)[SUBMIT MANUSCRIPT](#)[APC](#)

 **Vision:** The Journal of Biomedical Research & Environmental Sciences (JBRES) is dedicated to advancing science and technology by providing a global platform for innovation, knowledge exchange, and collaboration. Our vision is to empower researchers and scientists worldwide, offering equal opportunities to share ideas, expand careers, and contribute to discoveries that shape a healthier, sustainable future for humanity.

RESEARCH ARTICLE

Surface Characterization, Roughness Study Using Surface Profilometer and Nanometer Imaging Resolution for Polymers

Nandigana VR Vishal*

206 Fluid Systems Laboratory, Department of Mechanical Engineering, Indian Institute of Technology, Madras, Chennai 600036, Tamil Nadu, India.

Abstract

We understand the surface roughness and the vertical height features of polymers using surface profilometer. We study 5 polymers that include polystyrene, transparent Polyethylene Oxide (PEO), translucent Polyethylene Oxide, Polyvinyl Chloride (PVC) and textile cloth polymers for the first time. We study the front and back side of the polymers. We study the non-print and print region for the textile. On the front side of the polystyrene the surface roughness is 3.14 μm . The transparent polyethylene oxide surface roughness is 14.98 μm . The translucent polyethylene oxide surface roughness is 0.32 μm . The polyvinyl chloride surface roughness is 0.28 μm . We perform Scanning Electron Microscopy (SEM) imaging from micrometer to nanometer resolution. Energy Dispersive Spectroscopy (EDS) on the materials are studied. We obtain the elements in each of the polymers. The chemical composition of the elements in the polymers are obtained. In the textile cloth we understand the density difference between the print and non-print regions.

Introduction

The advent of polymer technology are needed. Polymers are light weight, low cost and require low power consumption. The structure of the polymers are studied. There are progress on the fabrication methods of polymers. The elements in the polymer are studied using energy dispersive spectroscopy [1]. Basic measurements of the polymer are the weight and percentage of the elements. Recent studies are ongoing on polymers towards imaging to characterize the structure. The nanoparticle preparation provides the size of the particle using the scanning electron microscopy [2-4]. Surface roughness are studied to understand the tribology aspects of the polymers and materials [5-7]. The applications are many that include printing, energy [8-11] and battery [12,13]. The change in

*Corresponding author(s)

Nandigana VR Vishal, 206 Fluid Systems Laboratory, Department of Mechanical Engineering, Indian Institute of Technology, Madras, Chennai 600036, Tamil Nadu, India

Email: nandiga@zmail.iitm.ac.in


DOI: 10.37871/jbres2287

Submitted: 14 February 2026

Accepted: 04 April 2026

Published: 05 April 2026

Copyright: © 2026 Vishal NVR.

Distributed under Creative Commons CC-BY 4.0 

OPEN ACCESS

VOLUME: 7 ISSUE: 4 - APRIL, 2026



How to cite this article: Vishal NVR. Surface Characterization, Roughness Study Using Surface Profilometer and Nanometer Imaging Resolution for Polymers. J Biomed Res Environ Sci. 2026 Apr 05; 7(4): 18. Doi: 10.37872/jbres2287



the structure during the fabrication are yet to be explored. Surface profilometer provides the surface geometry of the said polymer [14,15].

The common elements in the polymer are organic, metals and alloys. The chemical elements are carbon, oxygen and hydrogen. The metals include sodium, lithium, potassium, aluminum, magnesium, copper and molybdenum [16]. For instance, polystyrene are produced from carbon, hydrogen and oxygen. Researchers have studied polystyrene from the ethylene and benzene hybridization fabrication methods [17]. Polystyrene are thermoplastics. They are opaque, durable, insulators and their dye monomers are easy to obtain by powder based manufacturing. They are used in CDs, toys, brush, packages, displays and insulators. Vibrational sum-frequency generation spectroscopy probes the molecules using force. They give the element composition in polystyrene. Numerical simulations on polymers to understand the molecules arrangement are available [18]. Polyethylene oxide are plastics that are used in batteries [19]. Their structure are different from polystyrene with the similar chemical elements that include the carbon, oxygen and hydrogen. The preparation of the polyethylene oxide using ethylene glycol, dye provides transparent and translucent surfaces. The knowledge of metal-polymer matrix on current are studied [20]. The nanoparticles in operando visualization are towards the measurement of the power. In the recent years polyethylene oxide with lithium are studied [21-24]. Polyvinyl chloride pipes are heavy use in pipe flow and agriculture irrigation. The elements in polyvinyl chloride are typical carbon, oxygen, hydrogen and chlorine. The fabrication of polyvinyl chloride from chemical vapor deposition are known [25,26]. The standard surface roughness parameters in polymers are studied using surface profilometer [27-32]. The cloth based polymers are investigated to understand the elements and surface roughness parameters [33-36].

In this paper, we study the five polymers that include polystyrene, transparent polyethylene oxide, translucent polyethylene oxide, polyvinyl chloride and textile cloth. We investigate the standard surface roughness parameters of our polymers for the first time. The surface roughness of the polystyrene with its high sensitivity to measure the material film are the novelty of the work. The surface roughness are characterized on the front and back side of the polystyrene. On the front side the surface roughness of polystyrene is $3.14 \mu\text{m}$ with the sensitivity of $0.01 \mu\text{m}$. These findings are available as coating surface using polystyrene on quartz [37]. The thickness mentioned from measurements of coated polystyrene are $6 \mu\text{m}$ that gives the new perspective on substrate polymer with quartz in measurements to alloys. We perform scanning electron microscopy on the polymers. We study the chemical elements and their composition on our polymers one by one using energy dispersive spectroscopy. The standard surface roughness parameters on the textile cloth are studied. We investigate the surface roughness on the non-print and print regions in the cloth.

The rest of the paper is outlined as follows. Section 2 discusses the materials and methods. A detailed discussion on the surface roughness of polymers are given in Section 3. Finally, conclusions are presented in Section 4.

Material and Methods

The scanning electron microscopy equipment are from IITM facility. The surface profilometer are available in IITM facility. We purchase the four polymers that include polystyrene, transparent polyethylene oxide, translucent polyethylene oxide and polyvinyl chloride from Lakshmi electrical and hardwares, India. The Computer Aided Design (CAD) drawing are made using freeform app. The drawings are provided to Sj Woven Labels, India. The textile cloth are purchased from Sj Woven Labels, India. The computer aided design drawings are printed on

the textile using woven label machine available in Sj Woven Labels, India. Table 1 shows the specification details and measurement conditions of the surface profilometer.

Results and Discussion

Figure 1 (a) shows the actual polystyrene. Figure 1 (b) shows 1 μm (c) 2 μm (d) 4 μm (e) 10 μm (f) 20 μm (g) 100 μm and (h) 200 μm imaging resolution. The scanning electron microscopy are used to image the polystyrene. Figure 1 (i) shows the materials present in the polystyrene. The elements are carbon, oxygen and calcium. The composition of carbon is 96.9 %, oxygen 2 % and calcium 1 %, respectively. We understand that the polystyrenes are organic clean polymers that have carbon and oxygen in majority.

Figure 2 (a) shows the front side of the

polystyrene. We define specific region to understand the vertical feature height and the surface roughness of the polystyrene polymer. Figure 2 (b) shows the contour of the defined region having surface area 4 mm by 4 mm. The contour shows the vertical height on the given surface area. The surface profilometer are used to obtain the standard surface roughness and parameters for polymers. Figure 2 (c) shows the 3D plot with the vertical feature height. There are surface heights. Figure 2 (d) shows the surface roughness along the 4 mm length. We obtain the approximate vertical height as 10.78 μm . We consider the value as average surface roughness. The number of points used to calculate the average surface roughness are 5. Table 2 shows the details of the polystyrene. Eq. (1) gives the root mean square value tabulated in table 2. We calculate the surface volume is $16 \times 10^{-11} \text{ m}^3$.

We calculate the the root mean square error (RMSE). The root mean square error is calculated as given in Eq (1).

$$RMSE = \sqrt{\frac{1}{n} \sum_{i=1}^n (|P_i - O_i|)^2} \quad (1)$$

Where P_i is the predicted value, O_i is the actual result for observation i. n is the number of data points.

The steps to calculate the root mean square error are given.

1. We first calculate the residuals (R). The residuals are obtained by calculating the absolute difference between the actual result and the predicted value. We avoid negative values in the answers because they are physical quantities.
2. We calculate the square of the residuals (R^2).
3. We calculate the mean squared error (MSE). We sum and mean of all the square of the residuals, respectively. We consider n is the total number of data points.

Name	Surface profilometer
View, capture and measure	Digital microscope
relevance to human task	Surface conditions of the material film in room temperature
Observation to image	Machine handles 50 mm by 50 mm surface area of the polymer. The thickness of material we use are 2 mm
3D measurement	Even when the target has an uneven surface, a fully-focused image is obtained instantly, composed from multiple images with varying focus positions. Additionally, the 3D display can be used to observe surface contours and roughness.
Noncontact, no damage on specimen	No preliminary preparation required. Simply place the sample on the stage and begin measurement.
High resolution scan the image to measure surface roughness	0.01 μm
Medium of scanning and imaging	Laser principle

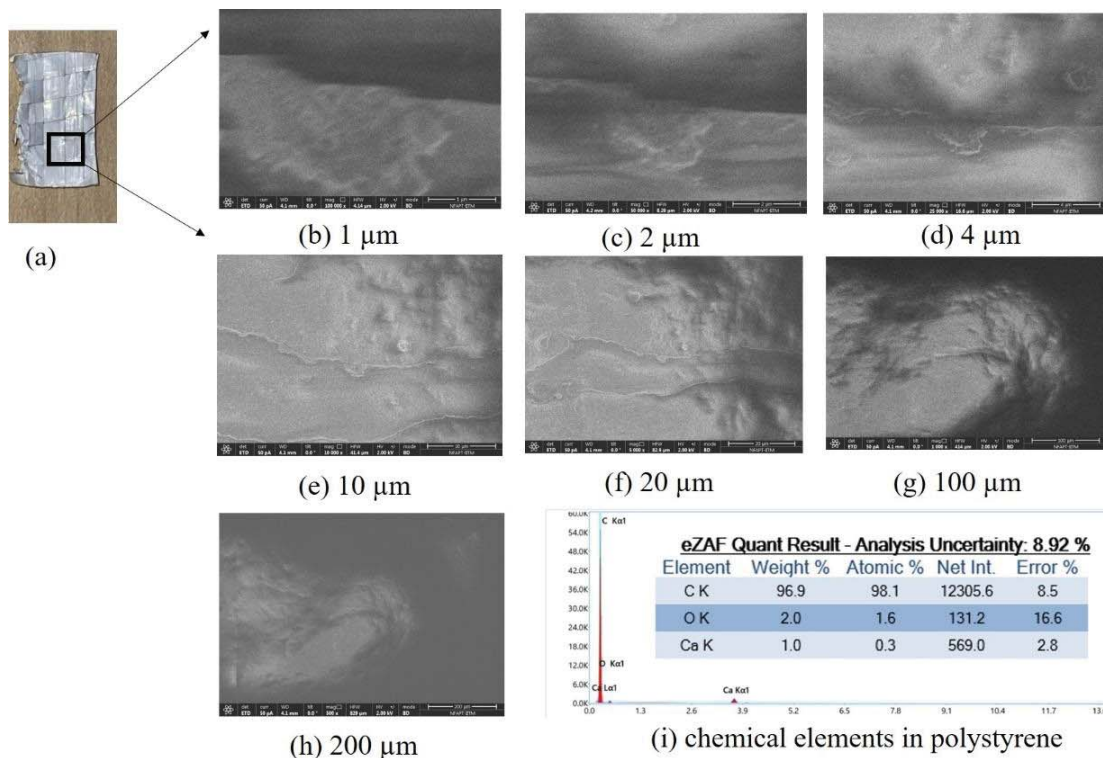


Figure 1 (a) Camera image of the actual polystyrene polymer. Scanning electron microscopy with image resolution (b) 1 μm (c) 2 μm (d) 4 μm (e) 10 μm (f) 20 μm (g) 100 μm (h) 200 μm and (i) energy dispersive spectroscopy to obtain the chemical elements in the polystyrene. The composition of carbon is 96.9 %, oxygen 2 % oxygen and calcium 1 %.

Table 2: Surface roughness characterization of the polystyrene.

x (mm)	y (μm)	average (μm)	residual (R)	residual (R ²)	MSE	RMSE
0.344828	-10.7805	10.78	0	0	29.78763	5.457804
0.413793	7.658537		3.12195122	9.746579		
1.151194	1.731707		9.048780488	81.88043		
2.944297	12.04878		1.268292683	1.608566		
3.002653	-18.2439		7.463414634	55.70256		

We calculate the root mean square error by taking the square root of the calculated mean square error.

Standard surface roughness parameters

- Surface roughness R_a

R_a is the most common parameter used in industry. R_a is the average vertical distance that the profile shown in figure 2 (d) deviates from the mean zero line. We use the region of 4 mm to calculate the surface roughness.

$$R_a = 1/n \sum_{(i=1)}^n |y_i| \quad (2)$$

$$R_a = \frac{1}{n} \sum_{i=1}^n |y_i| \quad (2)$$

• where n are the number of data points for the polystyrene polymer of length 4 mm. We consider 60 points. y_i are the vertical distance for each of the 60 points taken from figure 2 (d) using plot digitizer software. We understand the vertical distance in many points are very small $< 1 \mu\text{m}$, there are regions at 0.4 mm and 3 mm the vertical distance are $> 5 \mu\text{m}$. The surface roughness from Eq. (2) results in $3.14 \mu\text{m}$. We consider the surface roughness is higher.

Root mean square roughness R_q

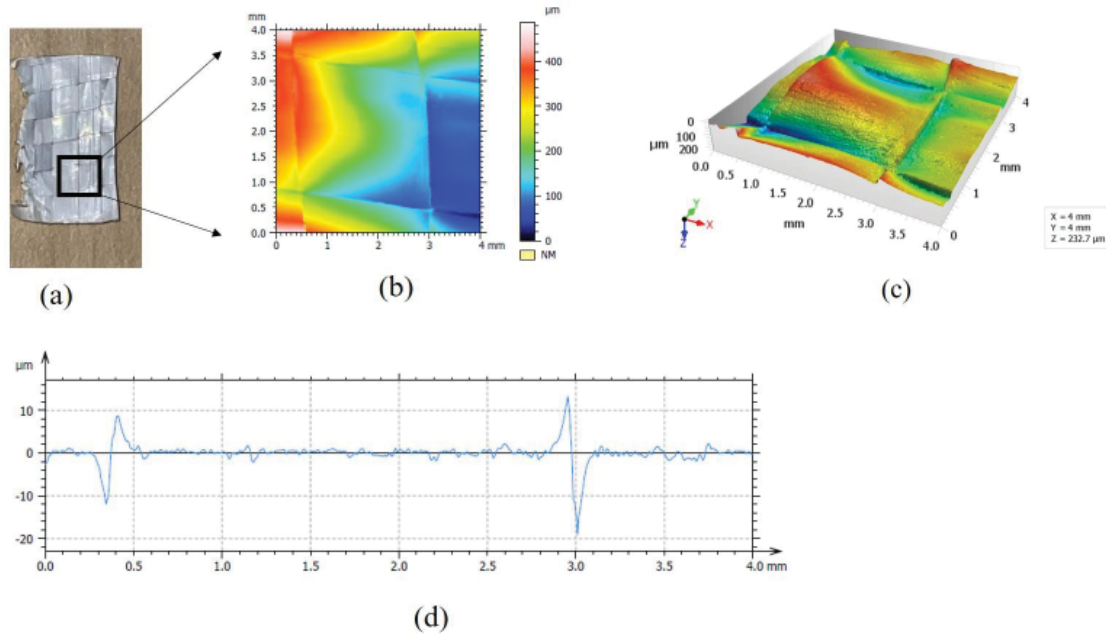


Figure 2 (a) Camera image of the front side of the polystyrene (b) contour from surface profilometer. We consider 4 mm by 4 mm surface area (c) 3D surface profile characteristics (d) line plot to obtain the standard surface roughness parameters in the selected area.

The root mean square roughness is calculated using Eq. (3).

$$R_q = \sqrt{\frac{1}{n} \sum_{i=1}^n y_i^2} \quad (3)$$

- The root mean square roughness on the front side of the polystyrene polymer is $5.19 \mu m$
- **Maximum Peak R_p**
- Maximum peak is the highest point on the surface roughness profile above the mean zero line as shown in figure 2 (d). It is denoted as R_p . The maximum peak surface roughness on the front side of the polystyrene is 12.5
- **Maximum Valley R_v**
- Maximum valley is the deepest point on the surface roughness profile below the mean zero line as shown in figure 2 (d). It is denoted as R_v . The maximum valley surface roughness on the front side of the polystyrene is $-18.25 \mu m$.
- **Total height R_t**

The total height is the sum of maximum

peak and maximum valley measurements. The total height are calculated using Eq. (4).

$$R_t = |R_p| + |R_v| \quad (4)$$

where R_t is the total height. The total height of the surface roughness on the front side of the polystyrene is $30.75 \mu m$. The surface roughness parameters on the front side of the polystyrene are tabulated in table 3.

Figure 3 (a) shows the back side of the polystyrene. The back side have small dull color owing to the scanning electron microscopy characterization. The front side of polystyrene are used to obtain the microscopy imaging. We define specific region to understand the vertical height of the back side of the polystyrene. Figure 3 (b) shows the contour in the region. The contour shows the vertical height. Figure 3 (c) shows the 3D plot with the surface uplift visible. Figure 3 (d) shows the surface roughness along the 4 mm length. The 1D, 2D and 3D should be validated with the consistent element model. That is the scope for the future. We obtain the

Table 3: Standard surface roughness parameters of the polymers.

Polystyrene front side	
Average surface roughness (R_b)	10.78 μm
Surface roughness (R_a)	3.14 μm
Root mean square roughness (R_q)	5.19 μm
Maximum Peak (R_p)	12.5 μm
Maximum Valley (R_v)	-18.25 μm
Total height (R_t)	30.75 μm
Polystyrene back side	
Average surface roughness (R_b)	2.5 μm
Surface roughness (R_a)	1 μm
Root mean square roughness (R_q)	1.48 μm
Maximum Peak (R_p)	6.01 μm
Maximum Valley (R_v)	-4.3 μm
Total height (R_t)	10.31 μm
Transparent polyethylene oxide non coated side	
Average surface roughness (R_b)	36.7 μm
Surface roughness (R_a)	14.98 μm
Root mean square roughness (R_q)	24.41 μm
Maximum Peak (R_p)	71.3 μm
Maximum Valley (R_v)	-26.67 μm
Total height (R_t)	97.97 μm
Transparent polyethylene oxide coated side	
Average surface roughness (R_b)	6.7 μm
Surface roughness (R_a)	2.45 μm
Root mean square roughness (R_q)	3.46 μm
Maximum Peak (R_p)	11.78 μm
Maximum Valley (R_v)	-6.01 μm
Total height (R_t)	17.79 μm
Translucent polyethylene oxide non coated side	
Average surface roughness (R_b)	0.68 μm
Surface roughness (R_a)	0.32 μm
Root mean square roughness (R_q)	0.39 μm
Maximum Peak (R_p)	0.86 μm
Maximum Valley (R_v)	-1.08 μm
Total height (R_t)	1.94 μm
Translucent polyethylene oxide coated side	
Average surface roughness (R_b)	4.53 μm
Surface roughness (R_a)	1.58 μm
Root mean square roughness (R_q)	2.1 μm
Maximum Peak (R_p)	7.27 μm
Maximum Valley (R_v)	-5.25 μm
Total height (R_t)	12.52 μm
Polyvinyl chloride front side	
Average surface roughness (R_b)	0.68 μm
Surface roughness (R_a)	0.28 μm
Root mean square roughness (R_q)	0.34 μm
Maximum Peak (R_p)	0.79 μm
Maximum Valley (R_v)	-0.74 μm

Total height (R_t)	1.53 μm
Polyvinyl chloride back side	
Average surface roughness (R_a)	4.76 μm
Surface roughness (R_s)	1.38 μm
Root mean square roughness (R_q)	2.4 μm
Maximum Peak (R_p)	10.32 μm
Maximum Valley (R_v)	-7.9 μm
Total height (R_t)	18.22 μm

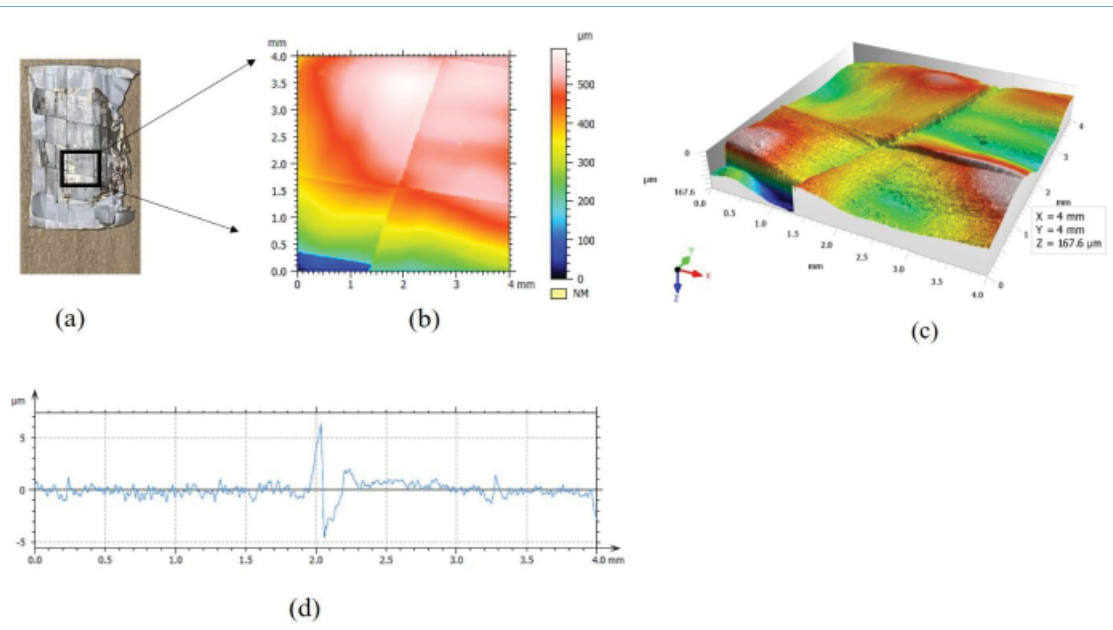


Figure 3 (a) Camera image of the back side of the polystyrene after the scanning electron microscopy imaging (b) contour from surface profilometer. We consider 4 mm by 4 mm surface area (c) 3D surface profile characteristics (d) line plot to obtain the standard surface roughness parameters in the selected area.

Table 4: Surface roughness characterization of the back side of the polystyrene.

x (mm)	y (μm)	average (μm)	residual (R)	residual (R^2)	MSE	RMSE
0.37234	0.195122	2.5	2.3	5.39	4.92	2.21
2.026596	5.902439		3.4	11.45		
2.06383	-4.34146		1.8	3.32		
2.207447	1.439024		1.081	1.17		
3.287234	0.707317		1.8	3.29		

approximate vertical height as 2.5 μm . Table 4 shows the average surface roughness same as vertical height. The number of points used here are 5. The surface volume is $4 \times 10^{-11} \text{ m}^3$.

The average surface roughness on the back side of the polystyrene polymer available in table 4 are 2.5 μm . The surface roughness on the back side of the polystyrene are 1 μm . The

root mean square roughness on the back side of the polystyrene polymer is 1.48 μm . The maximum peak surface roughness on the back side of the polystyrene is 6.01 μm . The maximum valley surface roughness on the back side of the polystyrene is -4.3 μm . The total height of the surface roughness on the back side of the polystyrene is 10.31 μm . The standard surface roughness parameters of polystyrene are given

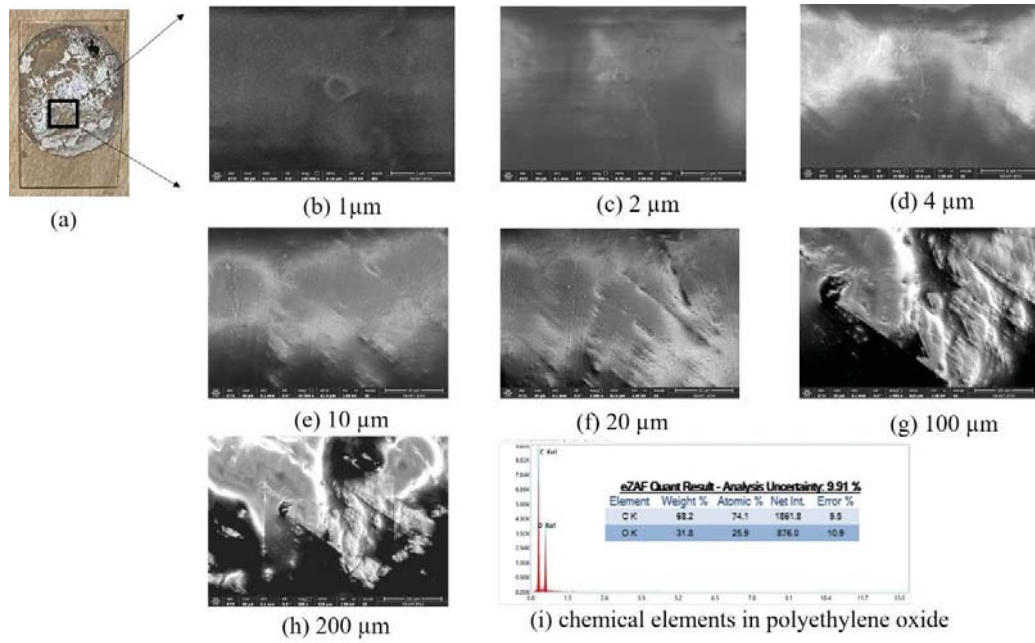


Figure 4 (a) Camera image of the actual transparent polyethylene oxide. Scanning electron microscopy imaging (b) 1 μm (c) 2 μm (d) 4 μm (e) 10 μm (f) 20 μm (g) 100 μm (h) 200 μm resolution and (i) energy dispersive spectroscopy to obtain the chemical elements in the transparent polyethylene oxide. The composition of carbon is 68.2 % and oxygen 31.8 %.

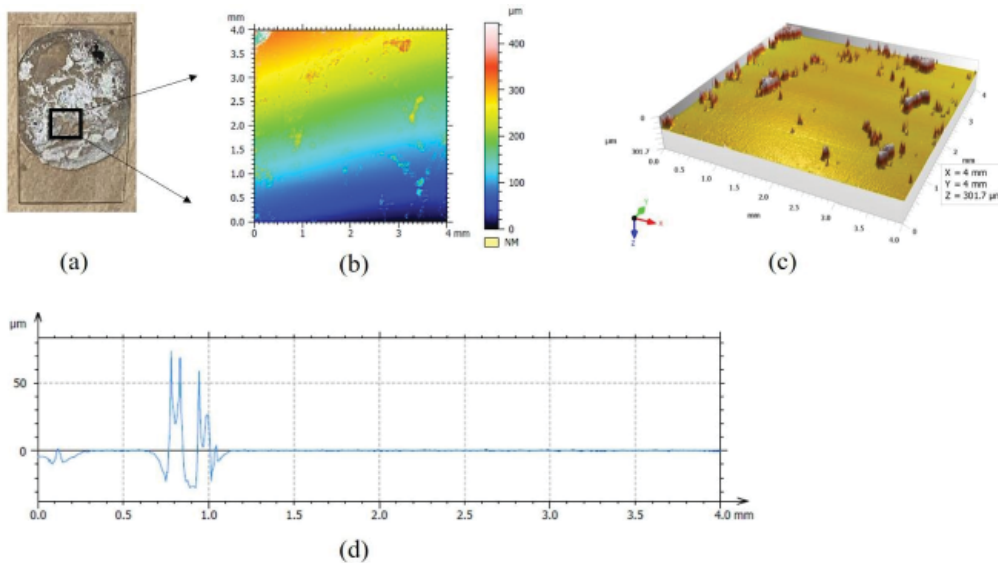


Figure 5 (a) Camera image of the non coated side of the transparent polyethylene oxide (b) contour from surface profilometer. We consider 4 mm by 4 mm surface area (c) 3D surface profile characteristics (d) line plot to obtain the standard surface roughness parameters in the selected area.

in table 3.

Figure 4 (a) shows the polyethylene oxide. Figure 4 (b) shows the 1 μm (c) 2 μm (d) 4 μm (e) 10 μm, (f) 20 μm, (g) 100 μm and (h) 200 μm resolution. Figure 4 (i) shows the materials

present in the polyethylene oxide. The materials are carbon and oxygen. The composition of carbon is 68.2% and oxygen is 31.8 %. The relation with the advanced new camera having microscopy features with the elements studied

Table 5: Surface roughness characterization of the transparent polyethylene oxide.

x (mm)	y (μm)	average (μm)	residual (R)	residual (R ²)	MSE	RMSE
0.140625	-8.26347	36.7	28.3	800.9	544.8	23.3
0.744792	-20.7784		14.9	222.6		
0.78125	69.46108		33.8	1139.8		
0.901042	-26.7066		8.9	80.9		
0.9375	57.60479		21.9	479.8		

Table 6: Surface roughness characterization of the coated side transparent polyethylene oxide.

x (mm)	y (μm)	average (μm)	residual (R)	residual (R ²)	MSE	RMSE
0.132626	-1.63975	6.7	5.1	25.9	13.1	3.6
0.228117	11.6646		4.9	24.7		
1.278515	6.63354		0.067	0.0045		
1.660477	9.540373		2.9	8.1		
2.758621	4.173913		2.5	6.4		

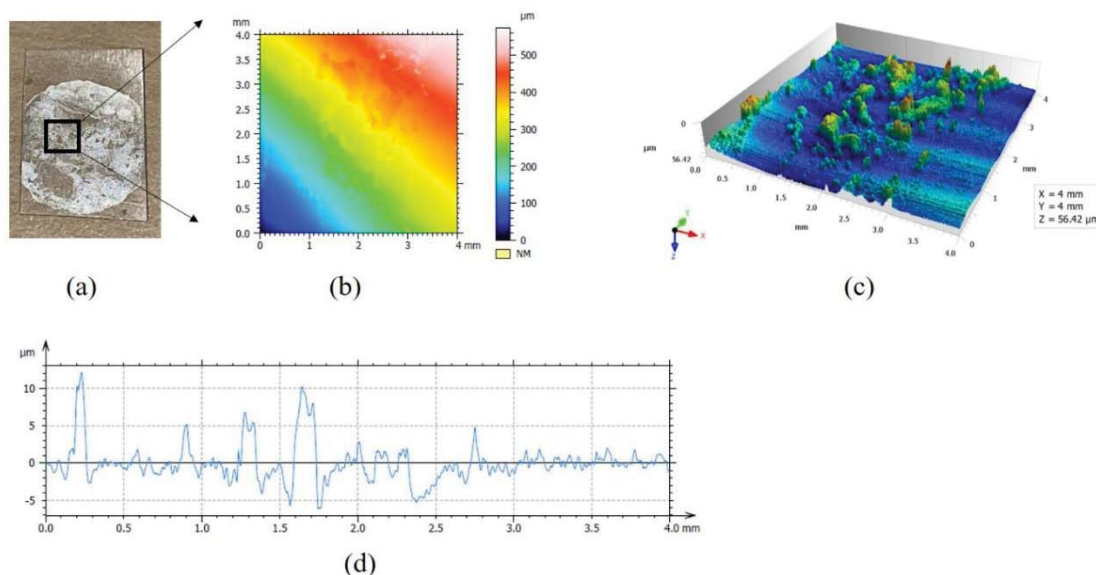


Figure 6 (a) Camera image of the coated side of the transparent polyethylene oxide after the scanning electron microscopy imaging (b) contour from surface profilometer. We consider 4 mm by 4 mm surface area (c) 3D surface profile characteristics (d) line plot to obtain the standard surface roughness parameters in the selected area.

in this paper needs further theory.

Figure 5 (a) shows the non-coated transparent polyethylene oxide. The non-coated by definition are the top surface that are used in the scanning electron microscopy machine. The coated regions are different. The coated regions are dull because they are resting with direct contact on the microscopy machine. To the non-coated transparent polyethylene oxide we define specific region to understand the vertical

feature. Figure 5 (b) shows the contour in the given region. The contour length is 4 mm and width is 4 mm. The contour shows the vertical height. Figure 5 (c) shows the 3D plot that have the ridges by definition some surface roughness regions. Figure 5 (d) shows the 1D line plot of the surface roughness along the 4 mm. We approximate the vertical height as 36.7 μm. The surface volume is $5.9 \times 10^{-10} \text{m}^3$.

Table 5 shows the average roughness is 37.6

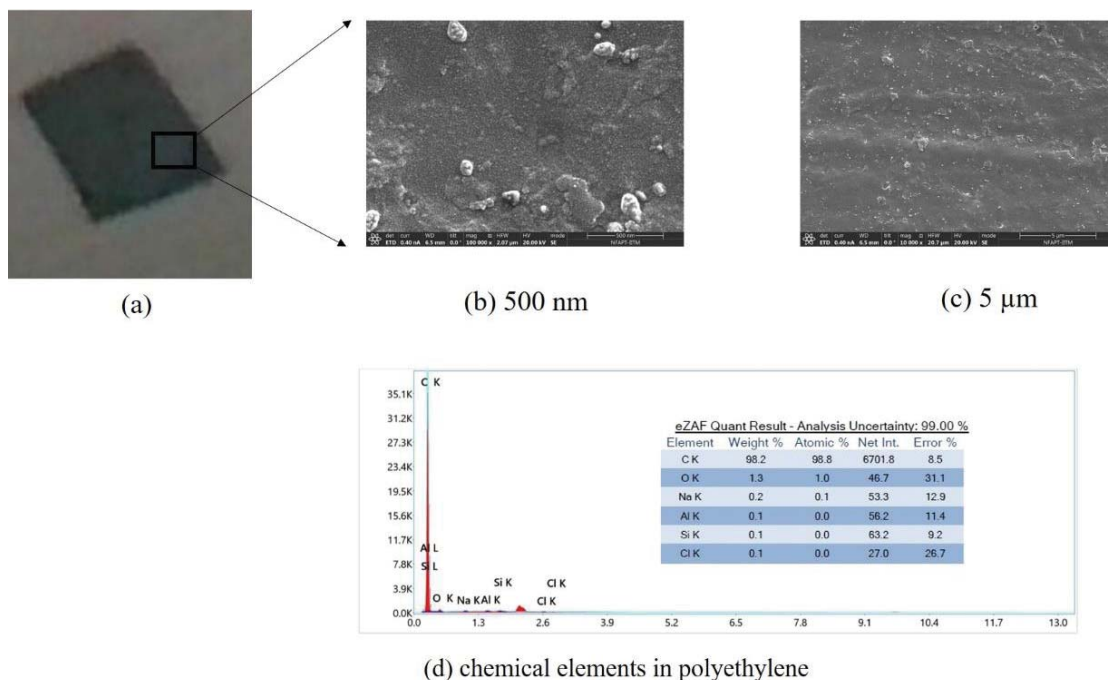


Figure 7 (a) Camera image of the actual translucent polyethylene oxide. Scanning electron microscopy imaging (b) 500 nm (c) 5 μm resolution and (i) energy dispersive spectroscopy to obtain the chemical elements in the translucent polyethylene oxide. The composition of carbon is 98.2 %, oxygen 1.3 %, sodium 0.2 %, aluminum 0.1 %, silicon 0.1 % and chlorine is 0.1 %.

Table 7: Surface roughness characterization of the non-coated side of the translucent polyethylene oxide.

x (mm)	y (μm)	average (μm)	residual (R)	residual (R ²)	MSE	RMSE
0.099738	0.354237	0.68	0.32	0.10	0.078	0.28
0.32021	-0.39153		0.29	0.083		
1.028871	0.666102		0.014	0.000193		
1.67979	-1.06949		0.39	0.152		
3.160105	0.89661		0.22	0.05		

μm. We believe the distance of objects and shape can be obtained from our polymer based sensor study. Table 3 shows the surface roughness for non-coated transparent polyethylene oxide. The table 3 reads the surface roughness on the non-coated side of the polyethylene oxide are 14.98 μm. The root mean square roughness is 24.41 μm. The maximum peak surface roughness is 71.3 μm. The maximum valley surface roughness is -26.67 μm. The total height of the surface roughness on the non-coated side of the polyethylene oxide is 97.97 μm. Figure 6 (a) shows the coated side of the polyethylene oxide. We define specific region to understand the vertical height. Figure 6 (b) shows the contour. The contour length is 4 mm and width

is 4 mm. The contour shows the vertical height. Figure 6 (c) shows the 3D plot. We observe the ridges at many instances. Figure 6 (d) shows the surface roughness along the 4 mm length. We approximate the vertical height as 6.7 μm. We calculate the surface volume is 1.1×10^{-10} m³.

Table 6 shows the vertical height on the coated side of the transparent polyethylene oxide. We consider 5 points. The average surface roughness are 6.7 μm. The surface roughness are 2.45 μm The root mean square roughness are 3.46 μm. The maximum peak surface roughness are 11.78 μm. The maximum valley surface roughness is -6.01 μm. The total height of the surface roughness on the coated side of the

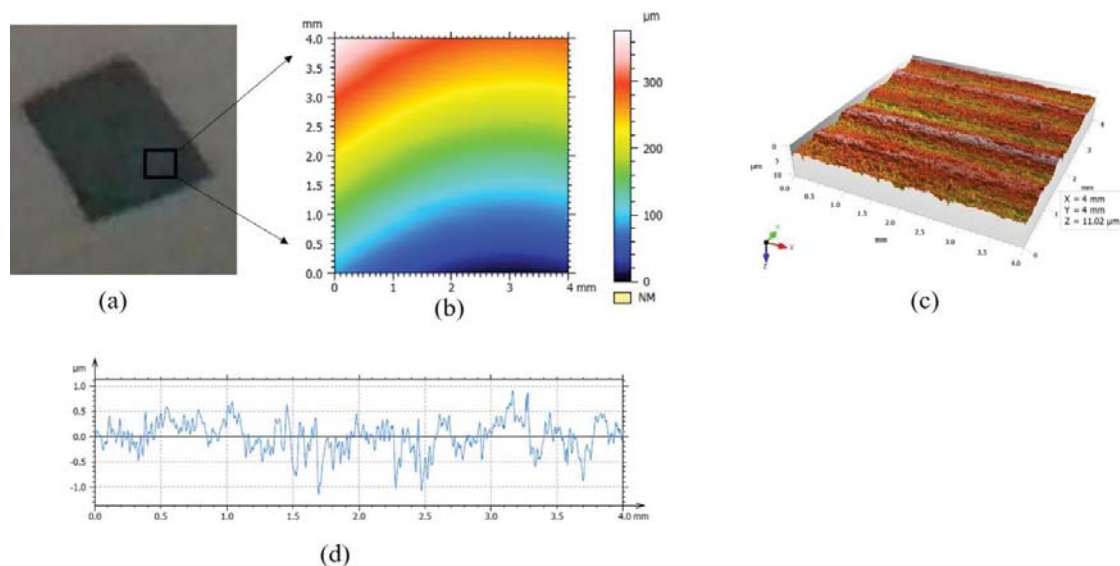


Figure 8 (a) Camera image of the non coated side of the translucent polyethylene oxide (b) contour from surface profilometer. We consider 4 mm by 4 mm surface area (c) 3D surface profile characteristics (d) line plot to obtain the standard surface roughness parameters in the selected area.

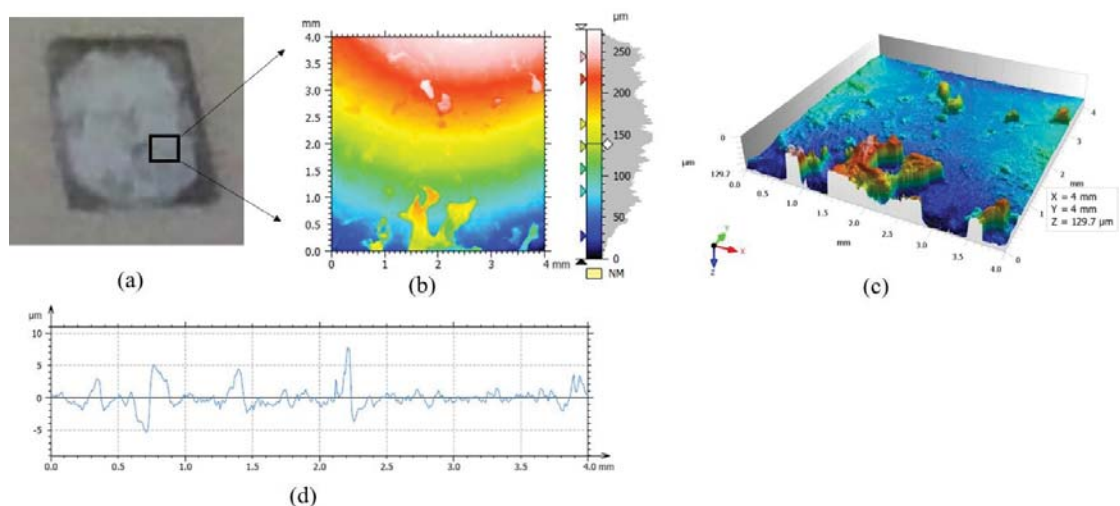


Figure 9 (a) Camera image of the coated side of the translucent polyethylene oxide after the scanning electron microscopy imaging (b) contour from surface profilometer. We consider 4 mm by 4 mm surface area (c) 3D surface profile characteristics (d) line plot to obtain the standard surface roughness parameters in the selected area.

polyethylene oxide are $17.79 \mu\text{m}$.

Figure 7 (a) shows the translucent polyethylene oxide (b) 500 nm and (c) 5 μm resolution. Figure 7 (d) shows the materials present in the translucent polyethylene oxide. The materials in the translucent polyethylene oxide are carbon, oxygen, sodium, aluminum, silicon and chlorine. The composition of

carbon is 98.2%, oxygen is 1.3 %, sodium 0.2%, aluminum 0.1 %, silicon 0.1 % and chlorine 0.1 %, respectively.

Figure 8 (a) shows the non-coated side of the translucent polyethylene oxide. The non coated region are used to image in the microscopy. The coated region is the resting surface during microscopy imaging. We define specific region

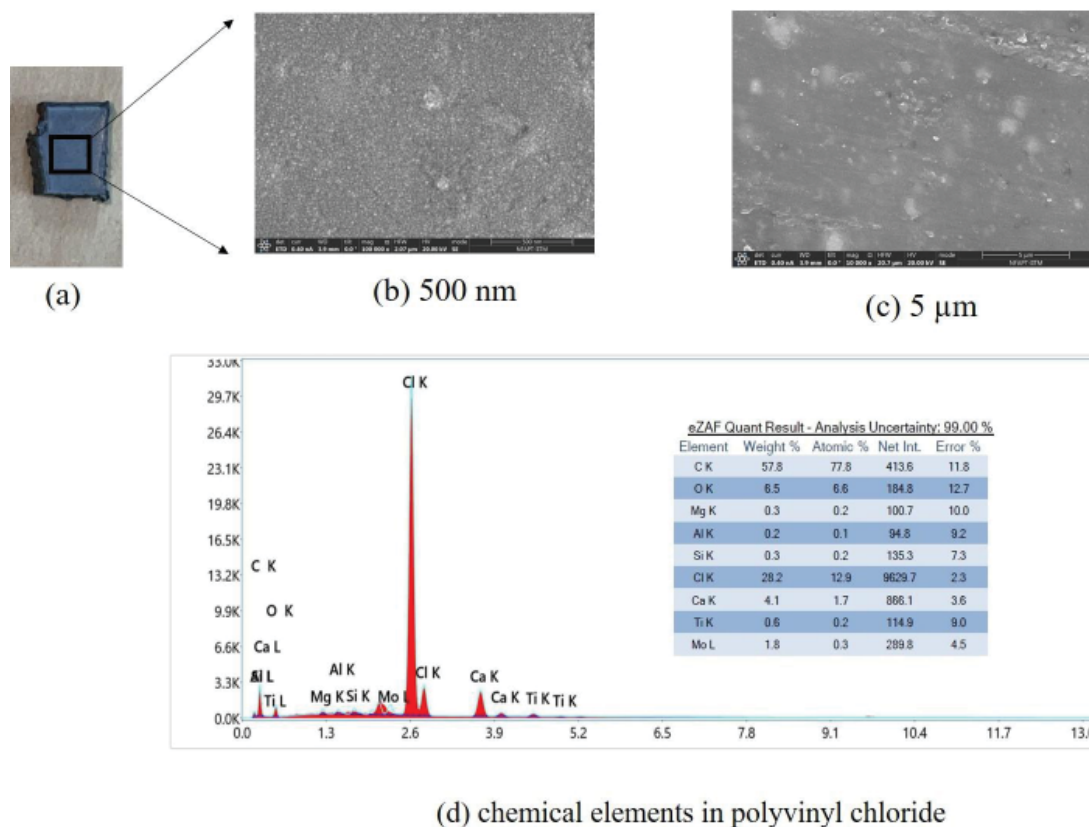


Figure 10 (a) Camera image of the actual polyvinyl chloride. Scanning electron microscopy imaging (b) 500 nm (c) 5 μm resolution and (i) energy dispersive spectroscopy to obtain the chemical elements in the polyvinyl chloride. The composition of carbon is 57.8 %, oxygen 6.5 %, magnesium 0.3 %, aluminum 0.2 %, silicon 0.3 %, chlorine 28.2 %, calcium 4.1 %, titanium 0.6 % and molybdenum 1.8 %.

to understand the vertical height. Figure 8 (b) shows the contour. The length of the contour is 4 mm and width is 4 mm. The contour shows the vertical height. Figure 8 (c) shows the 3D plot with ridge waves. Figure 8 (d) shows the 1D along the 4 mm line plot of the surface roughness. The surface volume is $1.1 \times 10^{-11} \text{ m}^3$. We approximate the vertical height as $0.68 \mu\text{m}$.

Table 7 shows the average surface roughness same as vertical height. We consider 5 points to obtain the average surface roughness. The value is $0.68 \mu\text{m}$. Table 3 shows the surface roughness parameters. The surface roughness of the non-coated polyethylene oxide are $0.32 \mu\text{m}$. The root mean square roughness is $0.39 \mu\text{m}$. The maximum peak surface roughness is $0.86 \mu\text{m}$. The maximum valley surface roughness is $-1.08 \mu\text{m}$. The total height of the surface roughness

on the non coated side of the translucent polyethylene oxide is $1.94 \mu\text{m}$. Figure 9 (a) shows the coated side of the translucent polyethylene oxide. We define specific region to understand the vertical height. Figure 9 (b) shows the contour in the region. The contour size have length 4 mm and width 4 mm. The contour shows the vertical height. Figure 9 (c) shows the 3D plot with surface heights. Figure 9 (d) shows the surface roughness along the 4 mm length. We approximate the vertical height as $4.53 \mu\text{m}$. We calculate the surface volume is $7.25 \times 10^{-11} \text{ m}^3$.

Table 8 shows the average surface roughness is $4.53 \mu\text{m}$. Table 3 shows the surface roughness of the coated polyethylene oxide are $1.58 \mu\text{m}$. The root mean square roughness is $2.1 \mu\text{m}$. The maximum peak surface roughness is $7.27 \mu\text{m}$. The maximum valley surface roughness is -5.25

µm. The total height of the surface roughness on the coated side of the translucent polyethylene oxide is 12.52 µm.

Figure 10 (a) shows the polyvinyl chloride. Figure 10 (b) shows the 500 nm and (c) 5 µm imaging resolution. Figure 10 (d) shows the materials present in the polyvinyl chloride. The composition of carbon is 57.8 %, oxygen is 6.5 %, magnesium 0.3 %, aluminum 0.2 %, silicon 0.3 %, chlorine 28.2 %, calcium 4.1 %, titanium 0.6 % and molybdenum 1.8 %, respectively.

Figure 11 (a) shows the front side of the polyvinyl chloride. The front side is used to image in the microscopy. We define specific region to understand the vertical height. Figure 11 (b) shows the contour. The contour length is 4 mm and width is 4 mm. The contour shows the vertical height. Figure 11 (c) shows the 3D plot to understand the surface roughness. Figure 11 (d) shows the 1D line plot along the 4 mm to observe the surface roughness. The surface volume is $1.1 \times 10^{-11} \text{ m}^3$. We approximate the vertical height as 0.68 µm.

Table 9 shows the average surface roughness same as the vertical feature is 0.68 µm. Table 3 shows the surface roughness is 0.28 µm The root mean square roughness is 0.34 µm. The maximum peak surface roughness is 0.79 µm.

The maximum valley surface roughness is -0.74 µm. The total height of the surface roughness on the front side of the polyvinyl chloride is 1.53 µm. Figure 12 (a) shows the back side of the polyvinyl chloride. The back side becomes coated side because the back side of the polyvinyl chloride are the resting side during the microscopy. The front side is used to image. We define specific region to understand the vertical height. Figure 12 (b) shows the contour. The contour have length 4 mm and width 4 mm. The contour shows the vertical height with shades. Figure 12 (c) shows the 3D plot. They have surface heights. Figure 12 (d) shows the surface roughness along the 4 mm length. The surface volume is $7.6 \times 10^{-11} \text{ m}^3$. We approximate the vertical height as 4.76 µm.

Table 10 shows the average surface roughness is 4.76 µm. Table 3 shows the surface roughness parameters. The surface roughness of the back side of the polyvinyl chloride is 1.38 µm The root mean square roughness is 2.4 µm. The maximum peak surface roughness is 10.32 µm. The maximum valley surface roughness is -7.9 µm. The total height of the surface roughness on the back side of the polyvinyl chloride is 18.22 µm. Here, we study textile cloth. We print the textile cloth with image. Figure 13 (a) shows the cloth polymer. The textile have print and non-print regions. We analyze the non-print region of the cloth. Figure 13 (b) shows the 5 µm (c) 10 µm (d) 30 µm (e) 50 µm (f) 100 µm (g) 300 µm and (h) 500 µm resolution. Figure 13 (i) shows the materials present in the non-printed cloth.

Table 8: Surface roughness characterization of the coated side translucent polyethylene oxide.

x (mm)	y (µm)	average (µm)	residual (R)	residual (R ²)	MSE	RMSE
0.346003	2.868132	4.53	1.67	2.76	2.51	1.59
0.712975	-4.93407		0.41	0.164		
0.760157	4.516484		0.014	0.000183		
2.21232	7.263736		2.74	7.48		
2.259502	-3.06593		1.47	2.15		

Table 9: Surface roughness characterization of the non-coated polyvinyl chloride.

x (mm)	y (µm)	average (µm)	residual (R)	residual (R ²)	MSE	RMSE
0.110236	-0.57086	0.68	0.101485714	0.010299	0.004507	0.067136
0.094488	0.711429		0.031428571	0.000988		
2.07874	0.736571		0.056571429	0.0032		
2.125984	-0.60857		0.071428571	0.005102		
3.19685	-0.73429		0.054285714	0.002947		

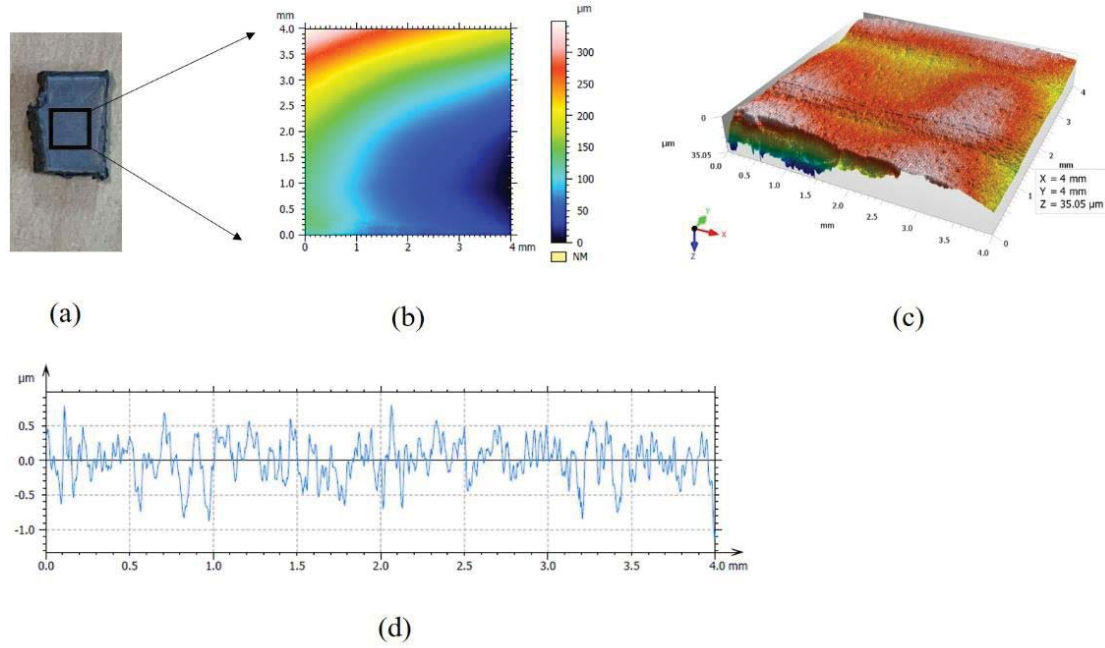


Figure 11 (a) Camera image of the front side of the polyvinyl chloride (b) contour from surface profilometer. We consider 4 mm by 4 mm surface area (c) 3D surface profile characteristics (d) line plot to obtain the standard surface roughness parameters in the selected area.

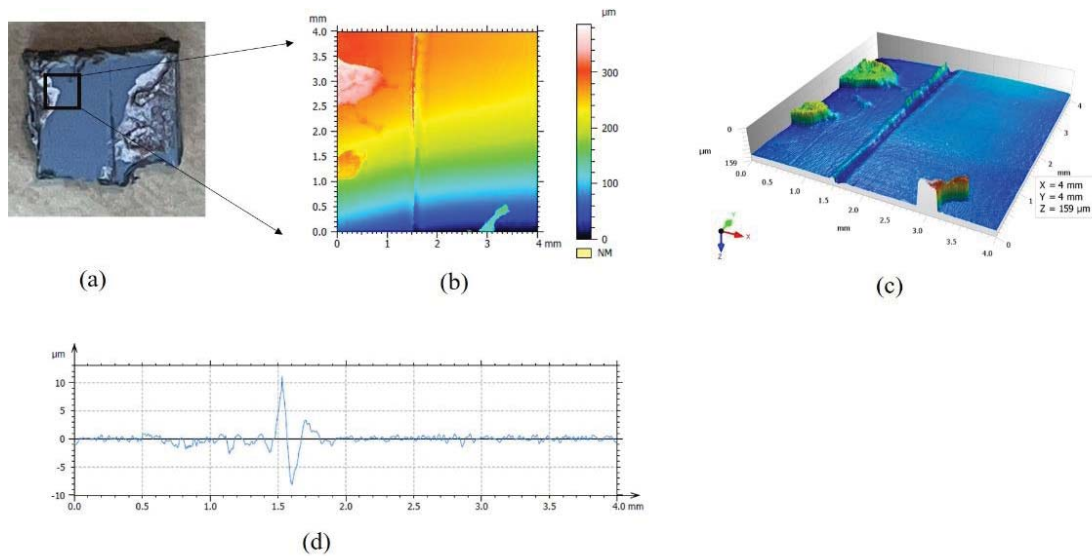


Figure 12 (a) Camera image of the back side of the polyvinyl chloride after the scanning electron microscopy imaging (b) contour from surface profilometer. We consider 4 mm by 4 mm surface area (c) 3D surface profile characteristics (d) line plot to obtain the standard surface roughness parameters in the selected area.

The materials are carbon, oxygen and copper. The composition of carbon is 74.7%, oxygen 15 % and copper 10.3 %. We observe distinct fibres and coils closely packed in the non-print area.

Figure 14 (a) shows the printed region in the

textile cloth. Figure 14 (b) shows the imaging in the printed region for 5 μm (c) 10 μm, (d) 30 μm, (e) 50 μm, (f) 100 μm, (g) 300 μm and (h) 500 μm resolution. Figure 14 (i) shows the materials present in the printed area of the cloth. The

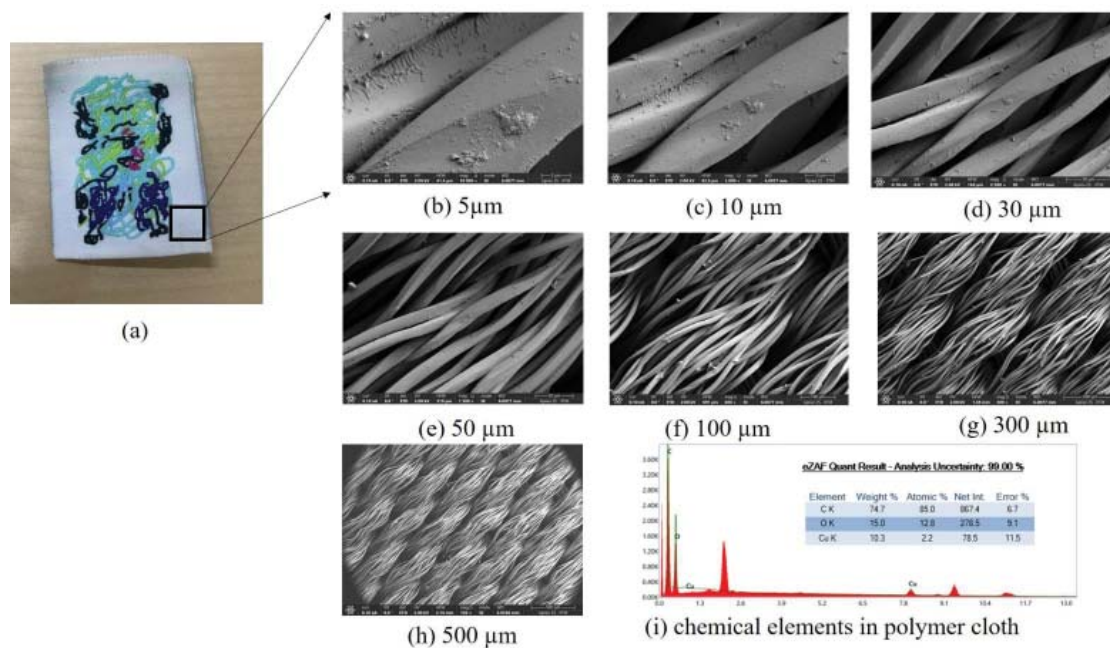


Figure 13 (a) Camera image of the textile cloth. We consider non print white region. Scanning electron microscopy with image resolution (b) 5 μm (c) 10 μm (d) 30 μm (e) 50 μm (f) 100 μm (g) 300 μm (h) 500 μm and (i) energy dispersive spectroscopy to obtain the chemical elements in the white region of cloth. The composition of carbon is 74.7 %, oxygen 15 % and copper 10.3 %.

Table 10: Surface roughness characterization of the back side of the polyvinyl chloride.

x (mm)	y (μm)	average (μm)	residual (R)	residual (R ²)	MSE	RMSE
0.557292	1.005376	4.76	3.75	14.03	13.02	3.61
1.145833	-2.20968		2.56	6.5		
1.536458	10.65054		5.9	34.7		
1.614583	-7.15591		2.4	5.75		
1.729167	2.736559		2.02	4.1		

Table 11: Polymers and their chemical elements with composition.

Polymers	Chemical elements with their composition
Polystyrene	Carbon (96.9%), Oxygen (2%) And Calcium (1%)
Transparent Polyethylene Oxide	Carbon (68.2%) And Oxygen (31.8%)
Translucent Polyethylene Oxide	Carbon (98.2%), Oxygen (1.3%), Sodium (0.2%), Aluminum (0.1%), Silicon (0.1%) And Chlorine (0.1%)
Polyvinyl Chloride	Carbon (57.8%), Oxygen (6.5%), Magnesium (0.3%), Aluminum (0.2%), Silicon (0.3%), Chlorine (28.2%), Calcium (4.1%), Titanium (0.6%) And Molybdenum (1.8%)
Non Print Region of the Textile	Carbon (74.7%), Oxygen (15%) And Copper (10.3%)
Print Region of the Textile	Carbon (77.9%), Oxygen (15.1%) And Copper (7%)

materials are carbon, oxygen and copper. The composition of carbon is 77.9%, oxygen 15.1 % and copper 7 %. We observe the difference of the structure in the print portion of the textile. We observe many fibres and coils with density arrangement prominent compared to the non-

printed cloth region. Table 11 shows the different polymers and their chemical elements with the composition. The polymers are front and back side of the polystyrene. We study coated and non-coated transparent polyethylene oxide, translucent polyethylene oxide and polyvinyl

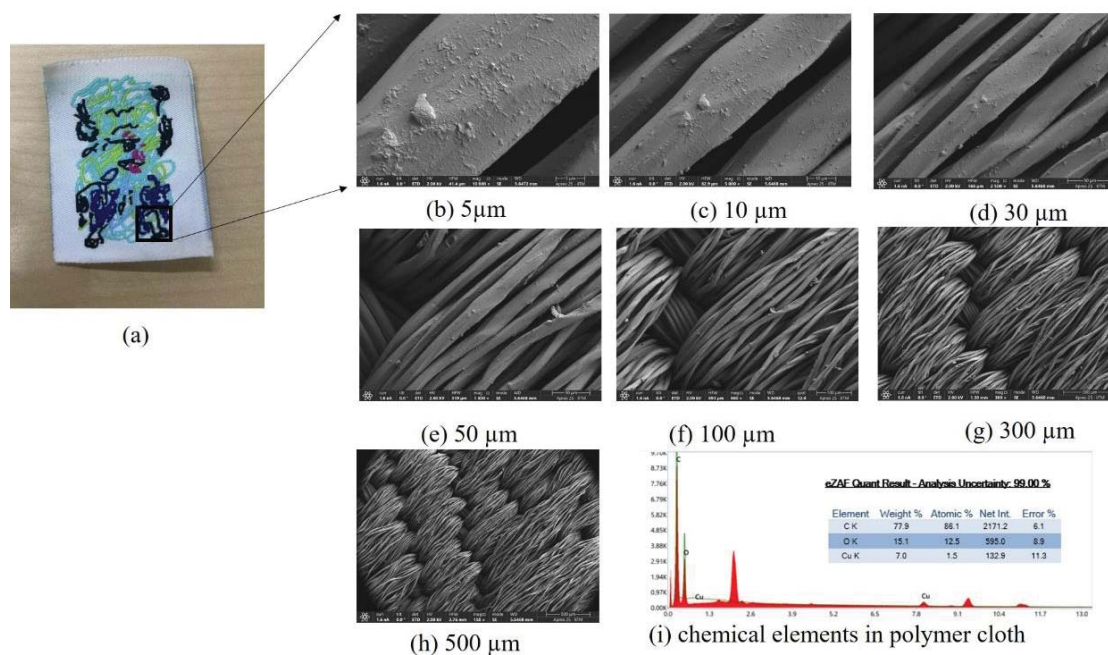


Figure 14 (a) Camera image of the textile cloth. We consider print indicated region. Scanning electron microscopy with image resolution (b) 5 μm (c) 10 μm (d) 30 μm (e) 50 μm (f) 100 μm (g) 300 μm (h) 500 μm and (i) energy dispersive spectroscopy to obtain the chemical elements in the print region of the cloth. The composition of carbon is 77.9 %, oxygen 15.1 % and copper 7 %.

chloride. We study non print and print region on the textile cloth.

Polystyrene exhibits average surface roughness of 10.78 μm on its front side and 2.5 μm on its back side. The molecular state of polystyrene provides the smooth structure during its usage. The surface roughness of the transparent polyethylene oxide is 36.7 μm . They have high surface roughness due to the preparation process of add the color. There could also be material consistency during the color addition to produce the transparent polyethylene oxide. The consistency in the preparation process resulted in low surface roughness in the translucent polyethylene oxide. The polymer chains in the translucent polyethylene oxide are packed together tightly and evenly. The polyvinyl chloride material is prepared using additive manufacturing process. Polyvinyl chloride are used in plumbing and housing pipes, which require highly uniform and smooth surfaces for efficient fluid transport

and insulation. The surface roughness in the textile cloth are driven by the fibrous geometry. The printed areas show more prominent arrangements of fibres and coils, suggesting that the addition of print material changes the gaps in the fabric. Thus, we observe surface roughness in the printed material cloth region in the measurement

Conclusion

To conclude we study polymers that include polystyrene, transparent polyethylene oxide, translucent polyethylene oxide, polyvinyl chloride and cloth. The cloth have print image on them. We use surface profilometer machine, scanning electron microscopy and energy dispersive spectroscopy. The surface profilometer provides the standard surface roughness parameters to our polymers. The imaging are done using microscopy. The chemical elements and their composition are obtained in our study. The predict ability of

the element composition in polymers using neural networks are scope for the future. We studied the density and structure on cloth with print images. Our work can find applications in sensors, geometry finding to materials, packaging, automobiles, pipe flow, coatings and printers.

Acknowledgment

There is no funding for this work.

Author contributions

Nandigana V. R. Vishal: Conceptualization, Data curation, Formal analysis, investigation, methodology, resources, software, supervision, validation, visualization, writing – original draft, writing – review and editing.

Conflicts of interest

The authors declare no conflict of interest.

Data availability

The data from the current study are available from the corresponding author upon reasonable request.

References

1. Ward IM, Sweeney J. Mechanical properties of solid polymers. 3rd ed. Chichester: John Wiley & Sons Ltd; 2013.
2. Wignall GD, Ballard DGH, Schelten J. Chain conformation in molten and solid polystyrene and polyethylene by low-angle neutron scattering. *J Macromol Sci B*. 1976;12:75-98.
3. Kik K, Bukowska B, Sicinska P. Polystyrene nanoparticles: Sources, occurrence in the environment, distribution in tissues, accumulation and toxicity to various organisms. *Environ Pollut*. 2020;262:1-9.
4. Anguissola S, Garry D, Salvati A, O'Brien PJ, Dawson KA. High content analysis provides mechanistic insights on the pathways of toxicity induced by amine-modified polystyrene nanoparticles. *PLoS One*. 2014;9:1-16.
5. Ghosh S, Knoblauch R, Mansori ME, Corleto C. Towards AI driven surface roughness evaluation in manufacturing: A prospective study. *J Intell Manuf*. 2025;36:4519-4548.
6. Nebot JVA, Pastor CV, Siller HR. A review of the factors influencing surface roughness in machining and their impact on sustainability. *Sustainability*. 2024;16:1917.
7. Chegdani F, Mansori ME, Bessonnet S, Pinault S. Comparative analysis of shape defects induced by the micro-machining of glassy polymers. *J Manuf Sci Eng*. 2024;146:1-12.
8. Tatek YB, Tsige M. Structural properties of atactic polystyrene adsorbed onto solid surfaces. *J Chem Phys*. 2011;135:174708.
9. Slooff LH, Kinderman R, Burgers AR, Bakker NJ, van Roosmalen JAM, Büchtemann A, et al. Efficiency enhancement of solar cells by application of a polymer coating containing a luminescent dye. *J Sol Energy Eng*. 2007;129:272-276.
10. Briggman KA, Stephenson JC, Wallace WE, Richter LJ. Absolute molecular orientational distribution of the polystyrene surface. *J Phys Chem B*. 2001;105(14):2785-2791.
11. Bzeih W, Gheribi A, Adams PMW, Hayes PL. Dependence of the surface structure of polystyrene on chain molecular weight investigated by sum frequency generation spectroscopy. *J Phys Chem C*. 2018;122(7):3838-3845.
12. Homann G, Stolz L, Nair J, Laskovic IC, Winter M, Kasnatscheew J. Poly(ethylene oxide)-based electrolyte for solid-state lithium batteries with high voltage positive electrodes: Evaluating the role of electrolyte oxidation in rapid cell failure. *Sci Rep*. 2020;10:1-9.
13. Blatt MP, Hallinan DT. Polymer blend electrolytes for batteries and beyond. *Ind Eng Chem Res*. 2021;60:17303-17327.
14. Terpiłowski K. Apparent surface free energy of polymer/paper composite material treated by air plasma. *Int J Polym Sci*. 2017;2017:1-8.
15. Guibert R, Lemesle J, Robache F, Bigerelle M. Roughness multiscale analysis of wear mechanisms in polymer abrasion. *Tribol Int*. 2026;214:1-15.
16. Lutz JF, Lehn JM, Meijer EW, Matyjaszewski K. From precision polymers to complex materials and systems. *Nat Rev Mater*. 2016;1:1-14.
17. Lenhart JL, Fischer DA, Chantawansri TL, Andzelm JW. Surface orientation of polystyrene based polymers: Steric effects from pendant groups on the phenyl ring. *Langmuir*. 2012;28:15713-15724.
18. Hall SA, Jena KC, Covert PA, Roy S, Trudeau TG, Hore



- DK. Molecular-level surface structure from nonlinear vibrational spectroscopy combined with simulations. *J Phys Chem B*. 2014;118:5617-5636.
19. Martinez JLO, Anastro AFD, Ibanez MM, Muller AJ, Mecerreyes D. Polyethylene oxide/sodium sulfonamide polymethacrylate blends as highly conducting single-ion solid polymer electrolytes. *Energy Fuels*. 2023;37:5519-5529.
20. Martinez JLO, Lingua G, Unanue L, Krol M, Ruokolainen J, Muller AJ, et al. Boosting ionic conductivity by ordering nanoparticles within all-polymer poly(ethylene oxide) nanocomposites. *ACS Polym Au*. 2025;5:488-493.
21. Kolesnikov TI, Voll D, Jeschull F, Theato P. Synthesis of polyimide-PEO copolymers: Toward thermally stable solid polymer electrolytes for lithium-metal batteries. *Eur Polym J*. 2024;217:113315.
22. St Onge V, Cui M, Rochon S, Daigle JC, Claverie JP. Reducing crystallinity in solid polymer electrolytes for lithium-metal batteries via statistical copolymerization. *Commun Mater*. 2021;2:1-11.
23. Mindemark J, Lacey MJ, Bowden T, Brandell D. Beyond PEO—alternative host materials for Li⁺ conducting solid polymer electrolytes. *Prog Polym Sci*. 2018;81:114-143.
24. Martinez JLO, Porcarelli L, Alegria A, Mecerreyes D, Muller AJ. High lithium conductivity of miscible poly(ethylene oxide)/methacrylic sulfonamide anionic polyelectrolyte polymer blends. *Macromolecules*. 2020;53:4442-4453.
25. Wilkes CE, Folt VL, Krimm S. Crystal structure of poly(vinyl chloride) single crystals. *Macromolecules*. 1973;6(2):235-237.
26. Pok S, Cigic IK, Strlic M, Rijavec T. Poly(vinyl chloride) degradation: Identification of acidic degradation products, their emission rates, and implications for heritage collections. *npj Herit Sci*. 2025;13:1-8.
27. Genna S, Leone C, Moretti P, Venettacci S. Influence of polymer surface roughness on the fractions of transmitted, reflected and absorbed energy in operation of laser transmission welding. *Lasers Manuf Mater Process*. 2024;11:469-491.
28. Ruzova TA, Haddadi B. Surface roughness and its measurement methods: Analytical review. *Results Surf Interfaces*. 2025;19:1-19.
29. Schmidt J, Thorenz B, Schreiner F, Dopfer F. Comparison of areal and profile surface measurement methods for evaluating surface properties of machined components. *Procedia CIRP*. 2021;102:459-464.
30. Jacobs TDB, Junge T, Pastewka L. Quantitative characterization of surface topography using spectral analysis. *Surf Topogr Metrol Prop*. 2017;5.
31. Pawar G, Pawlus P, Etsion I, Raeymaekers B. The effect of determining topography parameters on analyzing elastic contact between isotropic rough surfaces. *J Tribol*. 2013;135:1-10.
32. Persson BNJ. On the use of surface roughness parameters. *Tribol Lett*. 2023;71:1-9.
33. Machado TO, Stubbs CJ, Chiaradia V, Alraddadi MA, Brandolese A, Worch JC, et al. A renewably sourced, circular photopolymer resin for additive manufacturing. *Nature*. 2024;629:1069-1074.
34. Slusarczyk K, Flejszar M, Chmielarz P. Less is more: A review of μ L-scale of SI-ATRP in polymer brushes synthesis. *Polymer*. 2021;124:212.
35. Golhin AP, Tonello R, Frisvad JR, Grammatikos S, Strandlie A. Surface roughness of as-printed polymers: A comprehensive review. *Int J Adv Manuf Technol*. 2023;127:987-1043.
36. Kisiel K, Zaborniak I, Chmielarz P. Advances in the textile industry through surface-initiated reversible deactivation radical polymerization. *Polymer*. 2024;306.
37. Erasmus LJB, Poelman D, Smet PF, Terblans JJ, Swart HC. Processing and characterisation of polystyrene coatings and free-standing plates. *Opt Mater*. 2025;167:1-11.